

NAG5789

## NUMERICAL SIMULATION OF CUMULUS ENSEMBLES

Steven K. Krueger and Akio Arakawa

Dept. of Atmospheric Sciences, University of California  
Los Angeles, California 90024(NASA-CR-185088) NUMERICAL SIMULATION OF  
CUMULUS ENSEMBLES (California Univ.) 4 p

N89-71024

Unclas  
00/47 0213112

## 1. INTRODUCTION

Many important questions remain in the problem of cumulus parameterization. One of the most notable is what are the ensemble effects of mesoscale organization of cumulus convection? How do large-scale processes affect mesoscale organization, if at all? How strong is the coupling between large-scale and cloud-scale processes when mesoscale organization of clouds exists? To attempt to answer these questions, we are performing simulations using a numerical cumulus ensemble model. In particular, we are simulating a situation in which the imposed large-scale vertical velocity varies in time, and analyzing the results in terms of the cumulus ensemble's evolution and its relation to the large-scale forcing.

## 2. THE NUMERICAL MODEL

The numerical model is a two-dimensional cloud model based on the anelastic system of equations. It includes a third-order turbulence closure and a bulk microphysics parameterization.

Some results from an earlier version of the cumulus ensemble model were presented at the 16th Conference on Hurricanes and Tropical Meteorology (Krueger, 1985a). The earlier version of the model is fully described in Krueger (1985b). The current version differs in two major ways from the earlier version: (1) An ice-phase microphysical parameterization has been incorporated following Lord et al., (1984); and (2) the horizontal domain is larger (128 km). Both of these changes should make the development of mesoscale organization more likely than in the earlier version of the model.

The model domain is 18 km in depth. The vertical grid interval ranges from 100 m near the surface to about 1 km near the top of the domain. The horizontal grid interval is 1 km. The cyclic boundary condition is used in the horizontal direction; at the top and bottom, the boundaries are rigid. The lower boundary is assumed to be a sea surface.

## 3. THE NUMERICAL SIMULATION

## 3.1 External parameters

In the model, the large-scale vertical velocity ( $\bar{w}$ ), the radiative cooling rate, and the sea surface temperature are specified. During the first 24 hours,  $\bar{w}$  is zero. After hour 24,  $\bar{w}$  is positive at all levels with a maximum at a height of 7.5 km; its magnitude varies sinusoidally in time with a 48-hour period and reaches its maximum at hour 48 and every 48 hours thereafter. At 7.5 km,  $\bar{w}$  ranges between 0 and 5.5 cm/s. The radiative cooling rate is 2 K/day below 15 km and zero above 15 km. The sea surface temperature is fixed at 299.9 K.

To compute the surface fluxes, the surface wind speed ( $V$ ) is required. We set  $V=2.5$  m/s, which is typical for the ITCZ. To provide a decay mechanism for gravity waves, a radiative damping term is included in the equation for potential temperature ( $\theta$ ). We use  $-k(\bar{\theta}-\theta)$ , where  $\bar{\theta}$  is the horizontal average of  $\theta$ , and  $k=0.2 \text{ day}^{-1}$ .

Starting at hour 1, random perturbations are added to the potential temperature fields at two levels near the middle of the subcloud mixed layer to initiate cloud formation. The temperature perturbations range from -0.4 to +0.4 K. A different set of random temperature perturbations is used for each 5-minute interval. The perturbations are added evenly over each time interval and thus act as a perturbation heating or cooling.

## 3.2 Initial conditions

The initial sounding is in hydrostatic balance and follows the GATE Phase III mean sounding. The troposphere is moist and conditionally unstable below 4 km. The sounding was slightly modified to include a well-defined mixed layer 500 m deep. At the surface, the air is 1 K colder than the sea. All of the turbulence fields are zero initially.

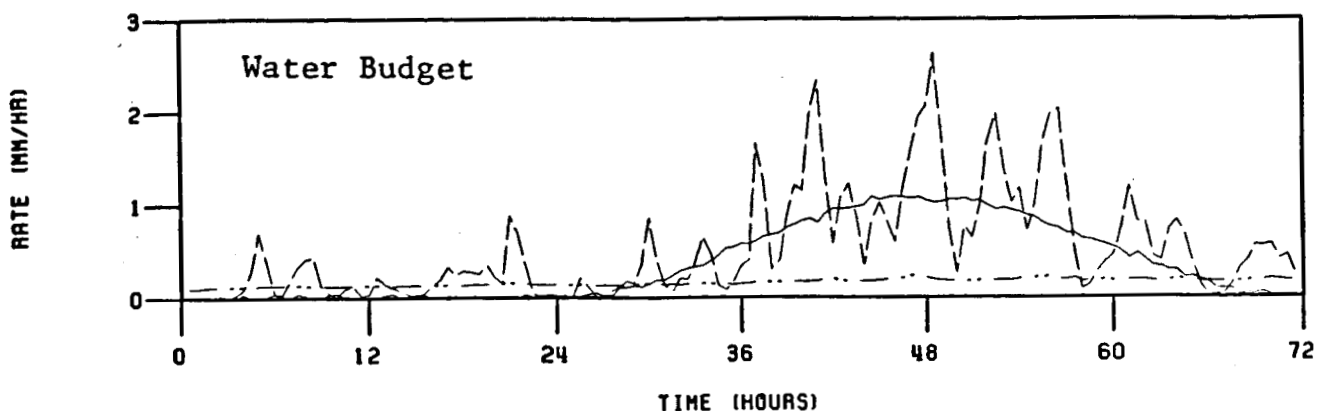


Fig. 1. Time series of the terms in the domain-integrated water budget: large-scale advection, solid line; surface evaporation rate, dash-dot line; surface rainfall rate, dashed line.

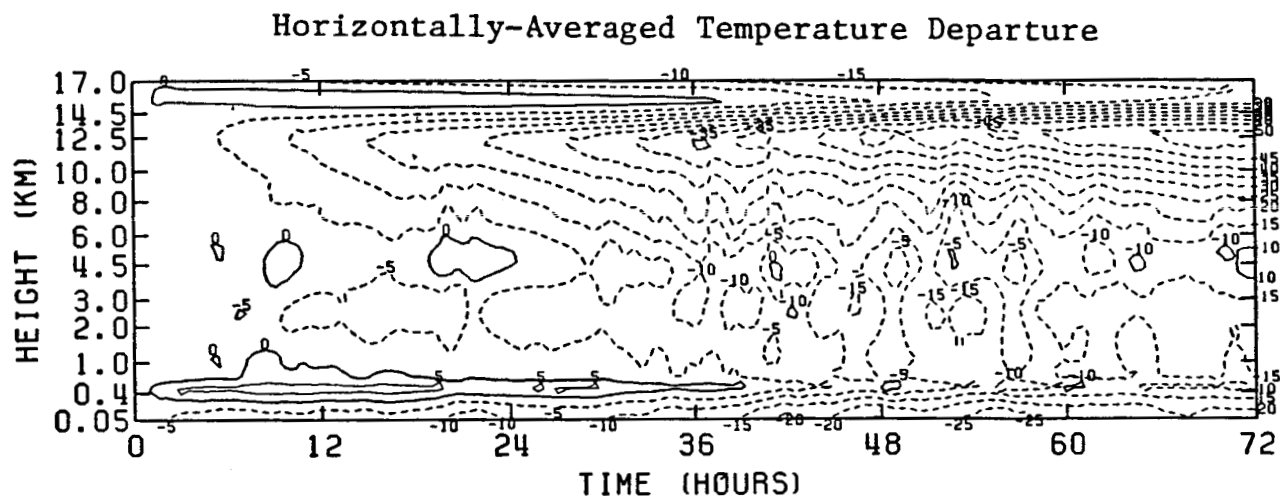


Fig. 2. Time series of  $\bar{T}$  shown as departure from initial  $\bar{T}$ . Contour interval is 0.5 K; dashed contours indicate negative departures. Contours are labeled in units of 0.1 K.

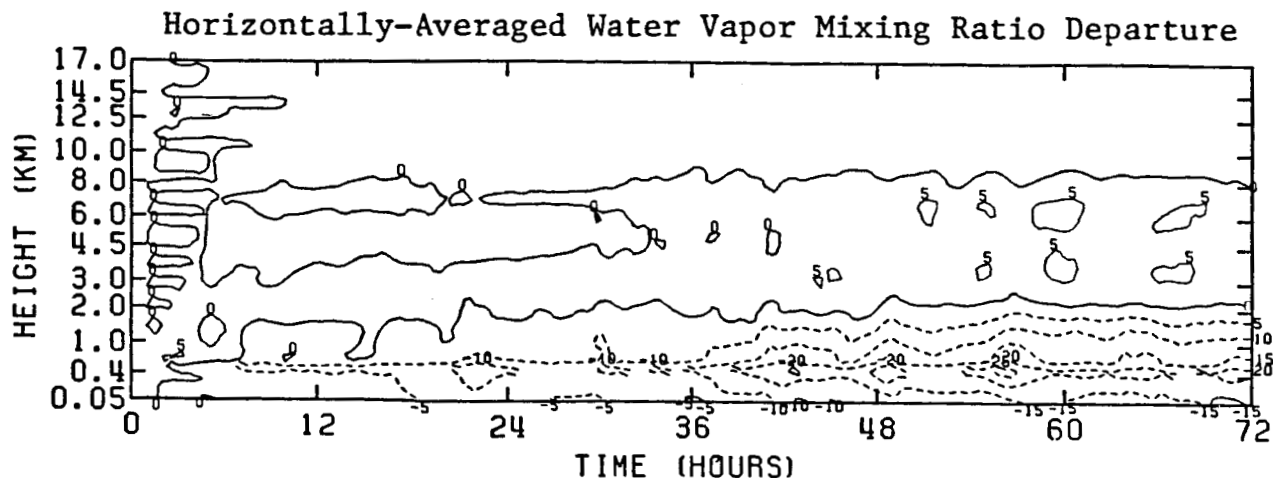


Fig. 3. Time series of  $\bar{q}_v$  shown as departure from initial  $\bar{q}_v$ . Contour interval is 0.5 g/kg; dashed contours indicate negative departures. Contours are labeled in units of 0.1 g/kg.

We are in the process of completing a simulation that will encompass several cycles of  $\bar{w}$ 's periodic variation. Preliminary results from the first 72 hours of this simulation follow. This period includes the initial 24-hour interval of zero  $\bar{w}$  followed by one complete 48-hour cycle.

$\bar{w} > 0$  tends to increase the moist convective instability—principally through adiabatic cooling ( $-\bar{w} d\theta/dz$ ) in the mid-troposphere. Therefore, we expect that convective activity will be related to  $\bar{w}$ .

During the first 36 hours, convective activity was relatively weak. This is evident in the time series of the surface rainfall rate, which is shown in Fig. 1, along with the other two terms in the domain-integrated water budget: the surface evaporation rate and the large-scale vertical advection,  $-\bar{w} dq/dz$ , where  $q_v$  is the horizontally-averaged water vapor mixing ratio. The period from hour 36 to hour 60 is particularly active. After hour 60, the convection subsides. The 24 hour period after

the maximum  $\bar{w}$  (and maximum  $-\bar{w} dq/dz$ ) at hour 48 is more active than the 24 hour period preceding hour 48.

Figs. 2 and 3 are time series of the horizontally-averaged temperature ( $\bar{T}$ ) and water vapor mixing ratio profiles shown as departures from their initial profiles. We see that the upper troposphere cools 5 K during the simulation; radiative cooling alone would cause a 6 K drop. The mid-troposphere cools much less—1 K at most—while the subcloud layer (SCL) cools by up to 2 K. The upper troposphere is strongly destabilized while the lower troposphere is stabilized.

Turning to  $q_v$  (Fig. 3) we see that the mid-troposphere is slightly moistened (by generally less than 0.5 g/kg) but the lower troposphere is dried by up to 2 g/kg. Note that both  $\bar{T}$  and  $q_v$  show a transition at around hour 36:  $\bar{T}$  decreases in the SCL and begins to fluctuate in the mid-troposphere;  $q_v$  decreases in the lower troposphere and increases slightly in the middle troposphere. These transitions are due to the onset of active convection.

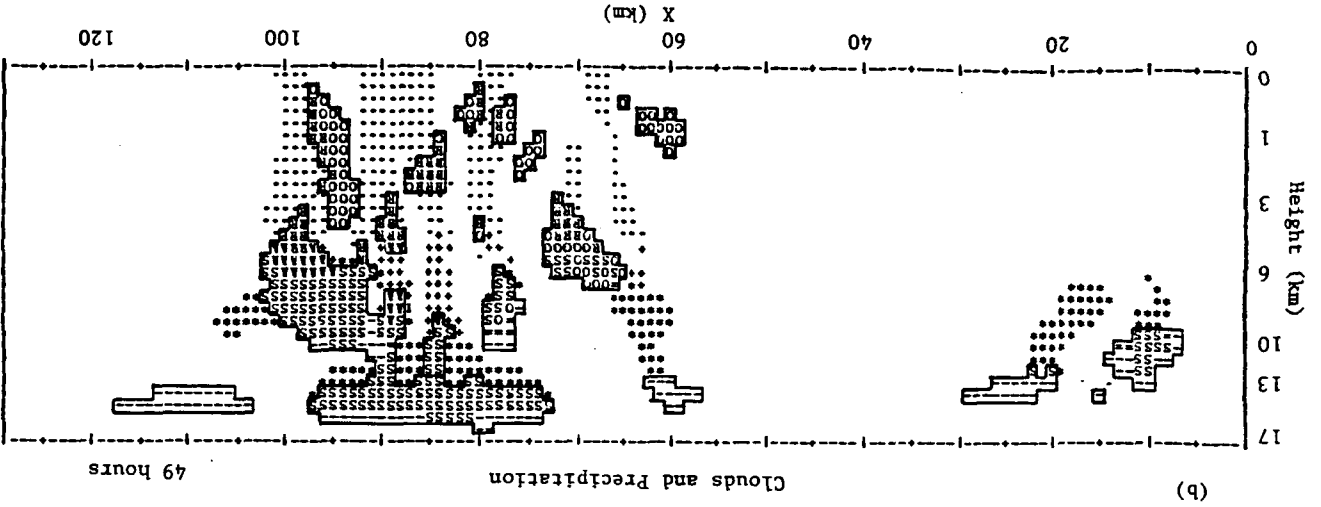
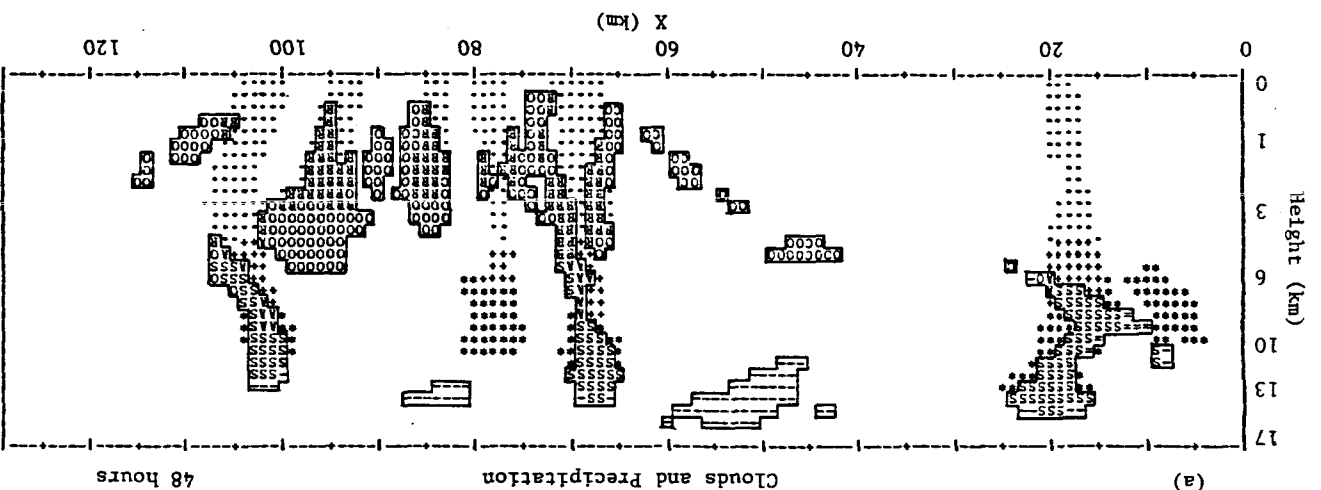


Fig. 4. X-Z sections showing distributions of clouds and precipitation at (a) hour 48 and (b) hour 49. Clouds are outlined. Symbols outside of clouds indicate precipitation with mixing ratio  $> 0.1$  g/kg; the symbol "R" indicates rain; "S", snow; "+", graupel; and "!", a mixture. Inside clouds, the symbol "R" indicates rain; "S", snow; "A", graupel; "O", cloud water only; "=", mixed cloud water and cloud ice only; and "-", cloud ice only.

Fig. 4 shows examples of the clouds and precipitation simulated by the model at hours 48 and 49. At hour 48 we see a decaying cell near  $x=20$  km and a group of cells extending from  $x=65$  to 105 km. One hour later, the cell at  $x=20$  km has further dissipated, while the cells in the group have coalesced somewhat and begun to dissipate.

Fig. 5 shows the temporal and spatial distribution of the surface rainfall intensity. From this figure, we see that the increase in convective activity after hour 36 is manifested in, on the average, more intense rainfall and a larger fraction of the area covered by rain. We also see that the rain-covered area is largely within a few groups of cells, especially from about hour 48 to hour 60. These groups were up to 40 km long and lasted several hours.

## 5. DETAILED ANALYSIS

### 5.1 Coupling between large-scale processes and cumulus ensembles

To what extent are the properties of a cumulus ensemble determined by the current large-scale processes? Among other things, the answer depends on the averaging scale. It probably also depends on the intensity of the convection and its degree of mesoscale organization. For example, the rainfall rate shown in Fig. 1 is a property of the cumulus ensemble; to what extent is it determined by large-scale processes?

The cumulus ensemble properties of most interest are  $Q_1$  and  $Q_2$ , the apparent heat source and apparent moisture sink due to cumulus convection. Using data from the simulation, we are calculating their time series and averaging each time series with respect to cycle phase. We can then obtain, and analyze, the variances of  $Q_1$  and  $Q_2$ .

We are also examining the quasi-equilibrium of the cloud work function. The cloud work function is a measure of the buoyancy generation of kinetic energy per unit cloud base mass flux; its quasi-equilibrium is one of the closure assumptions of the Arakawa-Schubert cumulus parameterization (Arakawa and Schubert, 1974).

### 5.2 Cloud-subcloud layer interaction

We are also extending the investigation of cloud-subcloud layer interaction by Krueger (1985). We are interested in the contributions to  $Q_1$  and  $Q_2$  by penetrative cumulus downdrafts and by rainfall evaporation. These effects are very important in the SCL, yet are difficult to include in a cumulus parameterization without introducing many additional disposable parameters.

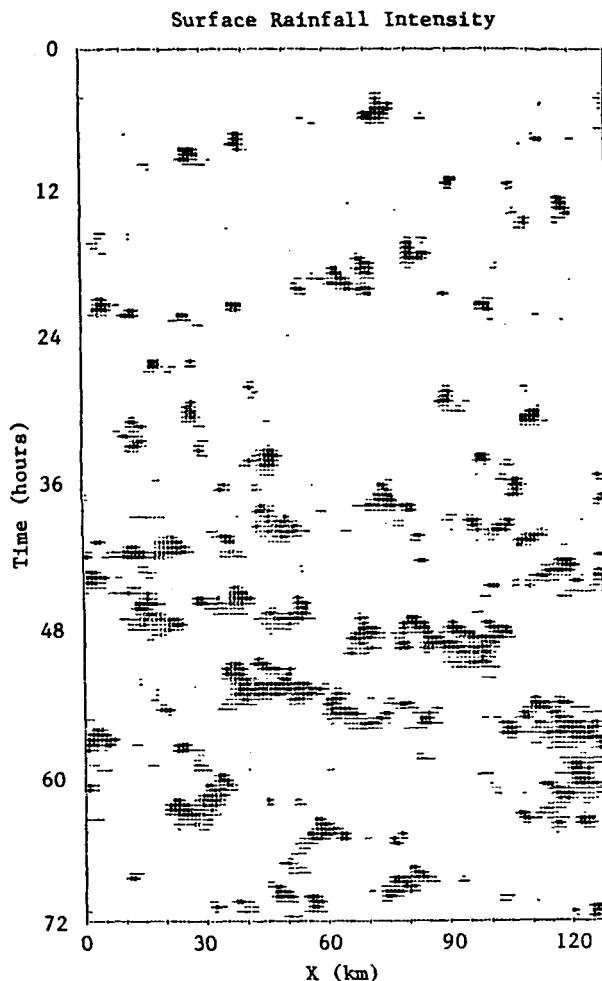


Fig. 5. Time series of spatial distribution of surface rainfall intensity. Degree of shading indicates rainfall intensity for rainfall rates  $> 0.25$  mm/hr averaged over 25 min. The peak rates were between 60 and 120 mm/hr averaged over 25 min.

## ACKNOWLEDGEMENT

Dr. Stephen J. Lord kindly provided the code for the ice-phase microphysical parameterization. This material is based upon work supported jointly by NSF and NOAA under Grant ATM-8515013 and by NASA under Grant NAG 5-789. Computing support was provided by the National Center for Atmospheric Research (NCAR), in Boulder, CO. NCAR is sponsored by NSF.

## REFERENCES

- Arakawa, A., and W. H. Schubert, 1974: The interaction of a cumulus ensemble with the large-scale environment, Part I. *J. Atmos. Sci.*, 31, 674-701.
- Krueger, S. K., 1985a: Numerical simulation of tropical cumulus clouds and their interaction with the subcloud layer. *Extended Abstracts, 16th Conference on Hurricanes and Tropical Meteorology*, Houston, Amer. Met. Soc., 25-26.
- Krueger, S. K., 1985b: Numerical simulation of tropical cumulus clouds and their interaction with the subcloud layer. Ph.D. Dissertation, Department of Atmospheric Sciences, University of California, Los Angeles. 205 pp.
- Lord, S. J., M. E. Willoughby and J. M. Piotrowicz, 1984: Role of a parameterized ice-phase microphysics in an axisymmetric, nonhydrostatic tropical cyclone model. *J. Atmos. Sci.*, 41, 2836-2848.